NIH Public Access
Author Manuscript
*Exp Cell Res*. Author manuscript; available in PMC 2009 June 10.

Published in final edited form as:
*Exp Cell Res*. 2008 June 10; 314(10): 2110–2122. doi:10.1016/j.yexcr.2008.03.008.

# Growth of cancer cell lines under stem cell-like conditions has the potential to unveil therapeutic targets

**Germana Rappa**, **Javier Mercapide**, **Fabio Anzanello**, **Lina Prasmickaite**, **Yaguang Xi**, **Jingfang Ju**, **Oystein Fodstad**, and **Aurelio Lorico**
*Mitchell Cancer Institute, University of South Alabama, Mobile, AL 36688*

## Abstract

Malignant tumors comprise a small proportion of cancer-initiating cells (CIC), capable of sustaining tumor formation and growth. CIC are the main potential target for anticancer therapy. However, the identification of molecular therapeutic targets in CIC isolated from primary tumors is an extremely difficult task. Here, we show that after years of passaging under differentiating conditions, glioblastoma, mammary carcinoma, and melanoma cell lines contained a fraction of cells capable of forming spheroids upon in vitro growth under stem cell-like conditions. We found an increased expression of surface markers associated with the stem cell phenotype and of oncogenes in cell lines and clones cultured as spheroids vs. adherent cultures. Also, spheroid-forming cells displayed increased tumorigenicity and an altered pattern of chemosensitivity. Interestingly, also from single retrovirally marked clones, it was possible to isolate cells able to grow as spheroids and associated with increased tumorigenicity. Our findings indicate that short-term selection and propagation of CIC as spheroid cultures from established cancer cell lines, coupled with gene expression profiling, represents a suitable tool to study and therapeutically target CIC: the notion of which genes have been down-regulated during growth under differentiating conditions will help find CIC-associated therapeutic targets.

### Keywords

cancer stem cells; cancer cell lines; glioblastoma; mammary carcinoma; melanoma

## INTRODUCTION

Conventional anticancer therapies may decrease the bulk of the tumor mass, mainly comprised of differentiated cancer cells, but are unlikely to result in long-term remissions if the minority of cancer-initiating cells (CIC), also named cancer stem cells, that feed tumor growth, are not targeted. CIC have been identified in leukemia [1,2], as well as in solid malignancies, including brain, breast, prostate, and lung cancer, and malignant melanoma [3–10]. In most cases, changes in expression of surface markers, such as CD133, CD24, CD44, Sca1 have allowed the identification of CIC. Also, the ability of some types of CIC to efflux the fluorescent dye Hoechst 33342 has been instrumental to CIC isolation, although the potential toxicity of the dye during fluorescence-based cell sorting has raised some concerns [11]. The tumorigenic

Corresponding Author: Dr. Aurelio Lorico, Mitchell Cancer Institute, University of South Alabama, 307 N. University Blvd., Mobile, AL 36688, USA, Tel. 251-461-1636, Fax: 251-460-6994, E-mail: E-mail: alorico@usouthal.edu.

**Publisher's Disclaimer:** This is a PDF file of an unedited manuscript that has been accepted for publication. As a service to our customers we are providing this early version of the manuscript. The manuscript will undergo copyediting, typesetting, and review of the resulting proof before it is published in its final citable form. Please note that during the production process errors may be discovered which could affect the content, and all legal disclaimers that apply to the journal pertain.

NIH-PA Author Manuscript
NIH-PA Author Manuscript
NIH-PA Author Manuscript

NIH-PA Author Manuscript

NIH-PA Author Manuscript

NIH-PA Author Manuscript

potential of CIC is generally assessed in xenograft models [4,7,12] or, when available, in syngeneic models [13,14], whose immune-competent microenvironment better mimics the clinical situation. CIC are potential targets for the development of molecular and pharmaceutical therapies to treat and prevent human cancer. The recent finding that targeting of the stem cell-associated protein CD44 eradicates human AML CIC [15] demonstrates that it is possible to target CIC by focusing on their stem cell properties rather than proliferation *per se*. However, technical issues, including tumor cell dissociation and sorting, hinder the process of isolating, expanding and analyzing CIC from human solid tumors [11].

Somatic stem cells in serum-free medium (SFM) form 3D-floating spheroid cell clusters, named neurospheres, mammospheres, oligospheres, mesospheres and others; spheroid structures with a stem cell-like phenotype have also been recently characterized from malignant tissues and cancer cell lines, and are increasingly used to study stem cell-like behavior [7,10, 14,16]. Here, we report that spheroid-forming cells, derived from established glioblastoma, mammary carcinoma and melanoma cell lines, display increased tumorigenicity, a gene expression profile consistent with CIC, and can be instrumental to the identification of cancer therapeutic targets.

## MATERIALS AND METHODS

### Cell culture

Murine GL-261 were cultured in Dulbecco's modified essential medium; human U87Mg glioblastoma; murine EMT6 and 4T1 mammary carcinomas; human MCF-7, MDA-MB-231, and MA-11 breast carcinomas; murine B16 and human FEMX-1 melanomas were cultured in RPMI-1640. For all the cell lines, medium was additioned with 10% fetal bovine serum. For spheroid formation, cells were enzymatically detached and plated at clonal density (300–500/cm2) in serum-free medium (SFM), consisting of Neurobasal-A medium (for GL-261, GL-261/DsRed2, U87Mg, and U87Mg/DsRed2) or D-MEM/F12 low osmolality medium for all the other cell lines (both from Gibco, Grand Island, NY) in the presence of B-27 supplement (Gibco, Grand Island, NY) and growth factors (1000 I.U./ml LIF for GL-261 and GL-261/DsRed2-cl.1, LIF + 10 ng/ml bFGF and 20 ng/ml EGF for U87Mg, U87Mg/DS-Red2-cl.1, MA-11, FEMX-1 and FEMX-1/eGFP-cl.1, bFGF and EGF for the others); in contrast to spheroid cultures derived from untransformed neural stem cells, the growth rate for all spheroid cultures derived from cancer cell lines was constant for over 6 months.

### Retroviral Vectors

pSF91-eGFP and pSF91-DsRed2 have a FMEV backbone [17]. To generate retroviral producers, the Phoenix-gp packaging cell line was transfected by the calcium phosphate/chloroquine method with the retroviral plasmid and a plasmid expressing the ecotropic or GALV glycoprotein as previously described [17]. In all the experiments, a MOI of 0.3 to 2 was used, to limit the expected integration frequency per cell to one or two. After transduction, the most fluorescent cells were sorted by flow cytometry, expanded in vitro, and cloned by limiting dilution. The growth rate and morphology of the clones selected were indistinguishable from those of their respective parental cell lines.

### Immunocytochemistry and flow cytometric analysis

For immunocytochemistry, cells were plated onto poly-L-lysine coated chamber slides, fixed in 4% paraformaldehyde, washed with PBS, permeabilized in 0.2% NP-40 and blocked with goat serum. The primary antibodies were obtained from Chemicon (Hofheim, Germany).

To analyze tumor cells ex-vivo without interference from normal contaminating cells, we employed the supravital DNA stain Hoechst 33342. All tumor cells investigated in the present

NIH-PA Author Manuscript

NIH-PA Author Manuscript

NIH-PA Author Manuscript

study have an hyperdiploid DNA content, which allows to exclude the diploid normal cell population of the host from the analysis. Hoechst 33342 (Calbiochem, La Jolla, CA) was prepared by dissolving into distilled water at a concentration of 1 mg/ml, sterilized by 0.22 μM filtration, and stored at 4°C. After mechanical dissociation of the excised tumors and passage through a 70-μm filter, cells were subsequently stained with 5 μg/ml Hoechst 33342, and with fluorescently conjugated monoclonal antibodies. Cells were analyzed using a 3-laser FACSVantage. 5 min before analysis, 5 μg/ml 7-AAD was added to each sample to exclude non-viable cells (7-AAD-positive).

After sterile sorting of cell sub-populations labeled with fluorescent antibodies, an aliquot of cells was routinely re-analyzed by flow cytometry to check for purity.

To compare the level of *c-kit* expression in GL-261 in vitro and ex-vivo, antibody concentration, cell concentration and flow cytometric parameters were maintained constant.

## Drug Sensitivity Assay

The drug sensitivity patterns of GL-261/adh and GL-261/sph were determined using the MTS/PMS microtiter plate assay, as previously described [18]. To avoid bias related to the different culture medium employed for GL-261/adh and GL-261/sph, both cell populations were plated in serum-additioned medium for the duration of the cytotoxicity experiment.

## Gene Expression Profiling

CodeLink Mouse Whole Genome Bioarray (Amersham Biosciences, Chandler, AZ) was used to generate gene expression profiles. A pool of 4 different cell preparations was used to extract RNA. To avoid bias related to the different culture medium employed for GL-261/adh and GL-261/sph, both cell populations were plated in serum-additioned medium for 24h before harvesting.

Total mRNAs were isolated using Trizol Reagent (Invitrogen, CA). cRNA synthesis was performed as per manufacturer's instructions. The fragmented cRNA was hybridized overnight at 37 °C in a shaking incubator at 300 rpm. After washings, and incubation with Cy5-streptavidin at room temperature for 30 minutes in the dark, arrays were washed, dried by centrifugation and kept in the dark until scanning. Images were captured on a GenePix 4200A scanner (Axon Instrument). The resulting image was quantified and the intensity of each spot divided by the median spot intensity to provide a scaled and comparable number across multiple arrays. After dot grid and QC, Codelink software generated export files for analysis by Genespring software, version 7.2. Normalization was applied in two steps: (a) "per chip normalization" in which each measurement was divided by the 50th percentile of all measurements in its array; and (b) "per gene normalization" in which all the samples were normalized against the specific samples (controls). Then data were filtered by flags with 4-fold cut-off. The expression profiles of the different groups were compared using one-way ANOVA with cut-off $p<0.05$. Of the total 35,290 genes present in the array, 10,371 were found expressed. We identified 266 significantly modulated genes (4-fold cut-off), with at least some annotated function. The down-regulated genes dominated, constituting 78 % of the modulated genes.

## Real-time PCR

To verify microarray data, TaqMan real-time PCR was performed for the selected genes, according to standard techniques. Gene expression relative to the endogenous control gene *glyceraldehyde-3-phosphate dehydrogenase* (*GAPDH*) was calculated as $2^{-\Delta\Delta Ct}$, where $\Delta\Delta C_t = \Delta Ct\,(GL261/sph) - \Delta Ct\,(GL261/adh)$. The $\Delta Ct$ values of GL-261/sph and the calibrator sample (GL261/adh) were determined by subtracting the average *Ct* value of the analyzed gene

NIH-PA Author Manuscript

NIH-PA Author Manuscript

NIH-PA Author Manuscript

from the average *Ct* value of the endogenous control gene GAPDH for each sample. The expression level of the analysed gene in the calibrator sample is equal 1. Relative quantification values $RQ=2^{-\Delta\Delta Ct}$ were plotted as a mean ± sd from three real-time PCR runs performed in duplicate.

### Tumor implantation

Animal studies were done under a protocol approved by the Institutional Animal Care and Use Committee. To establish i.c. tumors, GL-261 cells in 2 μL of medium were implanted stereotactically using a head frame (David Kopf Instruments, Tujunga, CA) in the brains of 6- to 8-week-old female C57BL/6 mice at the following coordinates: 1 mm anterior to the bregma, 2 mm lateral to the midline to a depth of 2 mm from the brain surface. After euthanasia, brains were removed and placed in cold 4% paraformaldehyde overnight, then sliced into 2 mm coronal sections prior to processing and embedding in paraffin. The tumors derived from Ds-Red2-tagged GL261 clones showed areas of necrosis, vascularity, nuclear pleomorphism, and mitotic figures, all features indistinguishable from the histopathology of parental GL-261 tumors as well as of human glioblastomas. For s.c. injection, cells were resuspended in 100 μl PBS, and injected into the right flank of the animals. 4T1/Ds-Red2, EMT6/Ds-Red2, GL-261/Ds-Red2 and FEMX-1/eGFP were all capable of growing in syngeneic mice with growth rates similar to the parental cell lines.

## RESULTS

### Cancer cell lines and clones contain a minor fraction of spheroid-forming cells

Upon 5 to 7-days culture in SFM, five human and four murine cancer cell lines, namely GL-261, U87Mg glioblastomas; EMT6, 4T1, MCF-7, MDA-MB-231, MA-11 mammary carcinomas; and B16 and FEMX-1 melanomas, formed non-adherent spheroids (Fig. 1A). Optimal growth as spheroids required leukemia inhibitory factor (LIF) and/or epidermal growth factor (EGF) plus basic fibroblast growth factor (bFGF) (Fig. 1B). LIF alone was more effective than EGF plus bFGF on GL-261 cells (Fig. 1B). The combination of LIF, EGF and bFGF was less effective than LIF alone, while stem cell factor alone was not able to support GL-261 growth as spheroids (Fig. 1B). For U87Mg, FEMX-1 and MA-11, optimal growth as spheroids in SFM was achieved in the presence of a combination of EGF, bFGF and LIF (Fig. 1B and data not shown), while optimal growth of EMT6, 4T1, MCF-7, MDA-MB-231 and B-16 in SFM was obtained in the presence of EGF and bFGF (not shown).

We then transduced GL-261, U87Mg and 4T1 cells with a Ds-Red2-expressing retroviral vector, and MCF-7 and FEMX-1 with an eGFP-expressing retroviral vector. Single-cell clones were isolated from each transduced cell culture by limiting dilution and expanded in vitro. After growth in SFM for 5–7 days, all clones formed spheroids, with efficiency analogous to those of their parental cell lines; the percentage of spheroid-forming cells for the different cell lines and their fluorescent clones ranged from 0.2 to 3.5% (Fig. 1A). After dissociation of spheroids and plating at clonal density in SFM, the percentage of spheroid-forming cells increased for all cell lines. Thus, for GL-261, 9.6% ± 0.76 of total cells (mean ± sd) formed secondary neurospheres. Subsequently, the spheroid-forming efficiency remained constant for at least three months. To further establish the stem cell model, we measured the colony-forming efficiency of these cell lines in serum-containing medium. In all cases, colony efficiency was much higher than spheroid-forming efficiency. We reasoned that if most of the colonies formed in serum were not derived from a “stem cell”, they should not be capable of forming sph colonies. In fact, after dissociation of the colonies grown in serum-supplemented medium into single cells and plating in SFM, the spheroid-forming efficiency was similar to that of the mass culture for each cell respective line; table 1 illustrates the results for a representative experiment for U87Mg, MA-11 and FEMX-1 cells. After 5 days of culture in SFM, the adherent cell

NIH-PA Author Manuscript

NIH-PA Author Manuscript

NIH-PA Author Manuscript

fraction (adh) and the non-adherent spheroid fraction (sph) of each of the 9 cancer cell lines were respectively detached or dissociated, and separately plated in standard serum-additioned medium for 5 additional days. All cultures resumed exponential growth. However, when re-plated in SFM, only the sph fractions reformed spheroids. The results of a representative experiment on MCF-7/eGFP cells are shown in Fig. 2A.

## Spheroid-forming cells express stem cell-associated surface markers

We found a differential expression of some surface markers associated with the stem cell phenotype in GL-261, U87Mg, 4T1, and MA-11 cultured in SFM as spheroids vs. adherent cultures. Immunocytochemistry revealed a significant increase (Student's t test, $p<0.05$) in the percentage of GL-261 cells expressing the neural stem cell-associated markers, nestin and A2B5, in spheroid cultures. Thus, nestin-positive cells increased from 19.3 ± 0.7 (SD) to 65.7 ± 16.2 (SD) and A2B5 increased from 38.9 ± 7.8 (SD) to 82.1 ± 12 (SD). No expression of the oligodendrocyte precursor marker, O4 was detected in any of the two cell types (not shown). The percentage of CD24− cells increased from 13.7 ± 2.5 (SD) to 87.9 ± 10 (SD) after culture of MA-11 in SFM for 7 days (Fig. 2B). Since 100% of MA-11 cells express CD44 (not shown), our data are in agreement with the recent identification of a CD44+CD24− breast CIC population [4]. Analogously, the percentage of CD44+CD24− cells increased from 73.9 ± 7 (SD) for U87Mg/adh to 98.7 ± 7 (SD) for U87Mg/sph. The percentage of cells expressing Sca1, a marker of mouse hematopoietic stem cells [19], was higher in 4T1/sph and in cells dissociated from s.c. tumors than in 4T1/adh; upon re-growth in adherent culture, the percentage of Sca1+ cells decreased (Fig. 2C).

To exclude that the heterogeneous expression of surface markers was due to the presence of multiple sub-populations in the cancer cell lines, we: (i) analyzed the expression of CD44 and CD24 in the clonal cell line U87Mg/Ds-Red-cl.1, and (ii) sorted by flow cytometry single Sca1-positive 4T1 cells based on their fluorescence and expanded them in culture. We found that (i) similarly to what found in parental U87Mg cells, the percentage of CD44+CD24− cells increased from 72 ± 6 (SD) for U87Mg/Ds-Red-cl.1/adh to 96.9 ± 5 (SD) for U87Mg/Ds-Red-cl.1/sph; (ii) after in vitro expansion, the clonal cell lines derived from Sca1-positive 4T1 cells had a heterogeneous expression of Sca1, including many Sca1-negative cells (Fig. 2C).

## Gene expression profiling of GL-261 spheroid-forming cells

To confirm that growth as spheroids resulted in selection of CIC, we searched for differential expression of genes associated with the stem cell phenotype in GL-261/sph and GL-261/adh. The global gene expression analysis of each sample was performed on a single microarray slide each with pooled quadruplicate samples, followed for representative genes by three real-time RT-PCR runs performed in duplicate. By whole genome microarray profiling, we found that only 56 genes with at least some annotated function were up-regulated in GL-261/sph (Supplementary Table 1). Among these was the *c-kit* gene, coding for the stem cell factor receptor. Up-regulation of *c-kit* in GL-261/sph was confirmed by flow cytometric analysis and real-time PCR (Fig. 3 and Suppl. Fig. 1). By simultaneous staining with the supravital DNA stain Hoechst 33342 and a *c-kit* antibody, we observed that the increase in *c-kit* expression was independent of the position of the tumor cells in the cell cycle (Fig. 3). Thus, *c-kit* was expressed in 72, 75 and 78% of GL-261/sph cells in G0/G1, S and G2M phase of the cell cycle vs. 11, 19 and 27% of GL-261/adh. We then analyzed *c-kit* expression in GL-261 cells dissociated from brain tumors of mice that had been implanted orthotopically with GL-261/adh or GL-261/sph. Based on the hyperdiploid DNA content of GL-261 cells, we removed all normal brain cells from the analysis. We observed that most cells from both GL-261/adh and GL-261/sph tumors expressed c-kit, at levels comparable with those of GL-261/sph cultured in vitro. Also for the ex-vivo cells, the expression of *c-kit* was independent of the position of the tumor cells in the cell cycle. Thus, c-kit was expressed in 93.9, 94.3 and 96.1% of ex-vivo GL-261/sph

NIH-PA Author Manuscript

NIH-PA Author Manuscript

NIH-PA Author Manuscript

cells in G0/G1, S and G2M phase of the cell cycle vs. 80.5, 81 and 85.3% of ex-vivo GL-261/adh. Additional oncogenes and stem cell-associated genes were found up-regulated, such as *nabc1* and *brca1*, reportedly expressed in NSC [20, 21], *trps-1* [22], three members of the *ras* oncogene family, *enpp2*, coding for autotaxin, a protein that reportedly contributes to glioblastoma cell motility and invasiveness [23], *sema3c*, implicated in tumorigenesis and tumor progression [24], the protein tyrosine phosphatase, receptor type, S (*ptprs*) gene, which is associated with neural stem cells [25], and the microtubule-associated protein tau (*mapt*), a marker of paclitaxel sensitivity [26]. Among the down-regulated genes was *numb*, implicated in the asymmetric division of stem cells, whose absence results in a rapid amplification of the stem cell pool, *timp3*, whose expression is inversely correlated with an aggressive cancer phenotype [27], *socs2*, reportedly not expressed in NSC [28], and the ephrin receptor *ephA2*, implicated in the differentiation of NSC [29]. Up- or down-regulation of several of these genes was confirmed by real-time PCR (Suppl. Fig. 1).

## Increased tumorigenic potential of spheroid-forming cells

We then compared the tumorigenic potential of GL-261/sph and GL-261/Ds-red2-clone1/sph with their respective adherent counterparts by orthotopic implantation of various cell inocula (Fig. 4). The intracerebral growth rate of $10^3$ enzymatically dissociated GL-261/sph or GL-261/DsRed2/sph was comparable with the growth rate of $10^5$ GL-261/adh. Immunostaining and morphometric quantification for the vascular marker CD31 revealed that both GL-261/sph- and GL-261/adh-derived tumors had a high microvessel density, with 26.8 ± 4.5 (SD) and 31.1 ± 5.6 (SD) microvessels/mm$^2$, respectively (Student's t test, not significant). Hematoxylin-eosin stained sections of brain tumors derived from adherent or spheroid GL-261 cultures showed highly infiltrating GL-261/sph tumors, compared with the more circumscribed tumors derived from GL-261/adh (Fig. 4A). Also U87Mg and FEMX-1 grown in SFM acquired increased tumorigenic potential compared with U87Mg/adh and FEMX-1/adh, respectively. Thus, the orthotopic implantation of $10^4$ U87Mg/sph or $10^5$ U87Mg/adh resulted after 20 days in a comparable intracerebral growth rate, while no tumor growth was observed after implantation of $10^4$ U87Mg/adh cells (Fig. 4B). Increased tumorigenicity for cells grown as spheroids was also observed for human FEMX-1 melanoma and MA-11 breast carcinoma cells. For both cell lines, after s.c. implant, the percentage of mice that developed a subcutaneous tumor >500 mm$^3$ was greater for cells grown as spheroid cultures (Fig. 4B).

## Spheroid-forming cells display an altered pattern of drug sensitivity

We then investigated whether the different gene expression profile resulted in a different pattern of chemosensitivity, as measured by an MTS/PMS microtiter plate assay after continuous exposure to the investigational drugs for 72h. Cells were exposed to the investigational drugs for 72 h. Consistent with Mapt overexpression, GL-261/sph cells showed a decrease in sensitivity to paclitaxel toxicity compared with GL-261/adh (Fig. 5e). The decreased sensitivity of GL-261/sph to paclitaxel was then confirmed by a clonogenic assay (Fig. 6). Contrary to what frequently reported for CIC, no over-expression of ABC transporters, including ABCG2, was detected in GL-261/sph (Suppl. Fig. 1 and Suppl. Table 1). Also, no side population (SP) was detected by flow cytometric analyses of Hoechst 33432-stained cells (not shown). Consistent with these findings, GL-261/sph did not display a multidrug resistance phenotype; rather, increased sensitivity to etoposide, melphalan and chlorambucil, and no change in sensitivity to the cytotoxic activity of doxorubicin (Fig. 5a–d). Fig. 5f shows that, presumably due to *c-kit* overexpression, GL-261/sph were less sensitive than GL-261/adh to imatinib mesylate (imatinib), a tyrosine kinase inhibitor in current clinical use [30–32]. No difference in sensitivity to imatinib was observed between U87Mg/adh and U87Mg/sph, which have a similar expression level of *c-kit* (not shown). Since imatinib does not penetrate the blood-brain barrier effectively [33], to assess the antitumor effect of imatinib in vivo, we implanted GL-261/adh and GL-261/sph s.c. instead of orthotopically. Imatinib was delivered

NIH-PA Author Manuscript

NIH-PA Author Manuscript

NIH-PA Author Manuscript

intraperitoneally once a day for 14 days at a dose of 50 mg/Kg. Consistent with the observation that *c-kit* expression is similar in tumors derived from GL-261/adh and GL-261/sph, we found that treatment with imatinib resulted in a similar growth delay on both tumors derived from GL-261/adh and from GL-261/sph (Fig. 5g).

## DISCUSSION

In the present paper, we provide evidence that after years of passaging under differentiating conditions, a fraction of each of nine tumor cell lines presents at least some of the original CIC properties. Our model of short-term selection and propagation of CIC as spheroid cultures in SFM from established cancer cell lines, coupled with gene expression profiling, represents a suitable tool to study and therapeutically target CIC: the notion of which genes have been down-regulated during growth under differentiating conditions may help find CIC-associated therapeutic targets. There are two possible interpretations of our results: (i) a complex phenomenon of "dedifferentiation" is stochastically triggered by a change in culture conditions, i.e. growth as spheroids in SFM in the presence of specific growth factors; this "dedifferentiation" process consists of activation of selected pathways and oncogenes and down-regulation of others, and results in ability to grow as non-adherent spheroids and increased tumorigenicity; (ii) the change in culture conditions selects a minor fraction of CIC, normally present in each cancer cell line. Our finding that the adherent cell fraction of cancer cell lines cultured under stem cell-like conditions is permanently unable to form spheroids in SFM strongly supports the second interpretation.

Interestingly, also from single retrovirally marked clones, it was possible to isolate cells able to grow as non-adherent spheroids in SFM and associated with increased tumorigenicity, suggesting that even a clonal tumor cell population is heterogeneous, with cells arrested at various stages of differentiation; presumably, only the least differentiated cells, or CIC, are then able to grow as non-adherent spheroids in vitro and give rise to tumors when transplanted in vivo.

The growth factor requirement for optimal growth as spheroids in SFM was different among the various cancer cell lines. LIF, known to maintain primitive mouse embryonic stem cells in an undifferentiated state [34], and to prevent senescence of human neural stem cells [35], was critical for spheroidal growth of several cell lines, including GL-261. It is intriguing that interleukin-6 and -11, and cardiotrophin-1, that have in common with LIF the gp130 receptor chain [36], were also able to promote GL-261 spheroidal growth. Although in our study in the presence of LIF and/or EGF and bFGF, the various tumor cell lines formed spheroids, displayed a gene expression profile consistent with CIC, and, in the case of GL-261, U87Mg, FEMX-1, and MA-11 increased tumorigenicity, the growth factor combinations employed were optimized for maximal spheroid formation, not maximal tumorigenicity. As all tumor cell lines employed in the present study are capable of forming tumors in syngeneic or immunodeficient mice, it will be possible to search for the growth factor combinations required for maximal tumorigenicity of each individual tumor cell line.

The isolation and expansion of CIC from human solid tumors to identify selectively expressed genes or pathways is an extremely difficult task [11]. Besides, it is conceivable that the process of isolation from the tumor stroma, sorting of the CIC population and their subsequent in vitro expansion result in profound changes in their expression profile. In the present study, we observed under spheroid culture an increased expression of genes which are well recognized potential targets of cancer therapy, such as *c-kit* [30] and CD44 [15], or genes associated with chemotherapy resistance, such as MAPT, as well as of many stem cell-associated genes, which are potential candidates as cancer therapy targets. *c-kit* is reportedly the most important marker of undifferentiated embryonic stem cells [37], and its gain-of-function mutations are associated

NIH-PA Author Manuscript

NIH-PA Author Manuscript

NIH-PA Author Manuscript

with several human neoplasms. Overexpression of *c-kit* in GL-261 spheroids was also reported in a recent study, that employed EGF and b-FGF instead of LIF to sustain serum-free growth [14]. Imatinib binds to an inactive conformation of *c-kit*, and competes with ATP for binding. Thus, imatinib resistance of GL-261/sph is presumably due to the increased expression of *c-kit*. It is conceivable that, as observed in vitro, also in vivo higher concentrations of imatinib or more potent inhibitors of *c-kit* would result in a greater antitumor activity than the modest effect observed in our experiments. However, imatinib displayed an equal antitumor potency in vivo on GL-261/sph and GL-261/adh tumors. We attribute this lack of differential effect to the equally high level of *c-kit* expression observed in both types of tumors. Our finding that GL-261/sph tumors have the same level of *c-kit* expression as GL-261/adh also suggests that *c-kit* expression is not associated with the infiltrative capacity. It should be stressed that c-kit is not uniquely associated with the CIC phenotype. In fact, for all the cell lines analyzed, the percentage of functionally-defined CIC within the bulk cell line population was in the range of approximately 0.2–3.5 percent (Figure 1A), while the fraction of cells that expressed stem cell-associated markers like c-kit (Figure 3) was over 50%.

The following observations exclude the possibility that our findings derive from an artificial in vitro phenomenon: (a) GL-261/sph and GL-261/Ds-red2-clone1/sph displayed a similar increase in tumorigenic potential. This finding excludes that the difference in tumorigenicity might be due to heterogeneity of the cancer cell line, for accumulations of mutations in long-term culture; (b) changes in expression profile and tumorigenic capacity normally occurred after a short time in culture (5–7 days); (c) before in vivo implantation, the spheroids were enzymatically dissociated into single cells; thus, the increased tumorigenicity of GL-261, U87Mg, FEMX-1, and MA-11 in SFM can not be attributed to their 3-D structure, but rather to their intrinsic cell properties; (d) the in vitro growth conditions and manipulations utilized in the present study for tumor spheroids are similar to those used for somatic stem cells in clinical protocols.

The clinical relevance of our findings is supported by the following observations: (a) In our study, we have found that human and murine spheroid-forming cells are very similar in their frequency and in their tumorigenic capacity; (b) GL-261, as well as most of the tumor cell lines employed in the present study, form tumors in vivo which are infiltrating and vascularized, and resemble human primary cancers; (c) formation of spheroids in serum-free medium by CIC isolated from patient's glioblastomas [7], medulloblastomas [10], and breast carcinomas [16,38] have recently been reported; (d) recent data demonstrate that CD44 can be effectively targeted by monoclonal antibodies in leukemic CIC [15].

Our data, together with the recent finding that GL-261 spheroids are better immunogens than the parental cell line for brain cancer immunotherapy [14], suggest that growth of cancer cell lines as spheroid-forming CIC can be efficiently used to investigate the antitumor effects of different therapeutic modalities, including chemotherapy, immunotherapy, gene therapy, radiotherapy, and anti-angiogenic therapy, and to develop drug screening strategies to selectively target CIC.

## Supplementary Material

Refer to Web version on PubMed Central for supplementary material.

## Acknowledgements

The authors wish to thank M.R. Boyd for his review of the manuscript, A. Sloan for helpful suggestions, R. Hester for flow cytometric analyses, J. King for comments on the histopathology, E. Hovig for help with microarray data analysis, and M. Alexeyev for help with preparation of retroviral vectors.

NIH-PA Author Manuscript

NIH-PA Author Manuscript

NIH-PA Author Manuscript

## References


1. Lapidot T, Sirard C, Vormoor J, Murdoch B, Hoang T, Caceres-Cortes J, Minden M, Paterson B, Caligiuri MA, Dick JE. A cell initiating human acute myeloid leukaemia after transplantation into SCID mice. Nature 1994;367:645–8. [PubMed: 7509044]
2. Bonnet D, Dick JE. Human acute myeloid leukemia is organized as a hierarchy that originates from a primitive hematopoietic cell. Nat Med 1997;3:730–7. [PubMed: 9212098]
3. Kim CF, Jackson EL, Woolfenden AE, Lawrence S, Babar I, Vogel S, Crowley D, Bronson RT, Jacks T. Identification of bronchioalveolar stem cells in normal lung and lung cancer. Cell 2005;121:823–35. [PubMed: 15960971]
4. Al-Hajj M, Wicha MS, Benito-Hernandez A, Morrison SJ, Clarke MF. Prospective identification of tumorigenic breast cancer cells. Proc Natl Acad Sci U S A 2003;100:3983–8. [PubMed: 12629218]
5. Lawson DA, Xin L, Lukacs RU, Cheng D, Witte ON. Isolation and functional characterization of murine prostate stem cells. Proc Natl Acad Sci U S A 2007;104:181–6. [PubMed: 17185413]
6. Li C, Heidt DG, Dalerba P, Burant CF, Zhang L, Adsay V, Wicha M, Clarke MF, Simeone DM. Identification of pancreatic cancer stem cells. Cancer Res 2007;67:1030–7. [PubMed: 17283135]
7. Singh SK, Clarke ID, Terasaki M, Bonn VE, Hawkins C, Squire J, Dirks PB. Identification of a cancer stem cell in human brain tumors. Cancer Res 2003;63:5821–8. [PubMed: 14522905]
8. Xin L, Lawson DA, Witte ON. The Sca-1 cell surface marker enriches for a prostate-regenerating cell subpopulation that can initiate prostate tumorigenesis. Proc Natl Acad Sci U S A 2005;102:6942–7. [PubMed: 15860580]
9. Fang D, Nguyen TK, Leishear K, Finko R, Kulp AN, Hotz S, Van Belle PA, Xu X, Elder DE, Herlyn M. A tumorigenic subpopulation with stem cell properties in melanomas. Cancer Res 2005;65:9328–37. [PubMed: 16230395]
10. Hemmati HD, Nakano I, Lazareff JA, Masterman-Smith M, Geschwind DH, Bronner-Fraser M, Kornblum HI. Cancerous stem cells can arise from pediatric brain tumors. Proc Natl Acad Sci U S A 2003;100:15178–83. [PubMed: 14645703]
11. Hill RP. Identifying cancer stem cells in solid tumors: case not proven. Cancer Res 2006;66:1891–5. [PubMed: 16488984]discussion 1890
12. Kondo T, Setoguchi T, Taga T. Persistence of a small subpopulation of cancer stem-like cells in the C6 glioma cell line. Proc Natl Acad Sci U S A 2004;101:781–6. [PubMed: 14711994]
13. Kruger JA, Kaplan CD, Luo Y, Zhou H, Markowitz D, Xiang R, Reisfeld RA. Characterization of stem cell-like cancer cells in immune-competent mice. Blood 2006;108:3906–12. [PubMed: 16912222]
14. Pellegatta S, Poliani PL, Corno D, Menghi F, Ghielmetti F, Suarez-Merino B, Caldera V, Nava S, Ravanini M, Facchetti F, Bruzzone MG, Finocchiaro G. Neurospheres enriched in cancer stem-like cells are highly effective in eliciting a dendritic cell-mediated immune response against malignant gliomas. Cancer Res 2006;66:10247–52. [PubMed: 17079441]
15. Jin L, Hope KJ, Zhai Q, Smadja-Joffe F, Dick JE. Targeting of CD44 eradicates human acute myeloid leukemic stem cells. Nat Med 2006;12:1167–74. [PubMed: 16998484]
16. Ponti D, Costa A, Zaffaroni N, Pratesi G, Petrangolini G, Coradini D, Pilotti S, Pierotti MA, Daidone MG. Isolation and in vitro propagation of tumorigenic breast cancer cells with stem/progenitor cell properties. Cancer Res 2005;65:5506–11. [PubMed: 15994920]
17. Lorico A, Bratbak D, Meyer J, Kunke D, Krauss S, Plott WE, Solodushko V, Baum C, Fodstad O, Rappa G. Gamma-glutamylcysteine synthetase and L-buthionine-(S, R)-sulfoximine: a new selection strategy for gene-transduced neural and hematopoietic stem/progenitor cells. Hum Gene Ther 2005;16:711–24. [PubMed: 15960602]
18. Lorico A, Rappa G, Finch RA, Yang D, Flavell RA, Sartorelli AC. Disruption of the murine MRP (multidrug resistance protein) gene leads to increased sensitivity to etoposide (VP-16) and increased levels of glutathione. Cancer Res 1997;57:5238–42. [PubMed: 9393741]
19. Suzuki N, Ohneda O, Minegishi N, Nishikawa M, Ohta T, Takahashi S, Engel JD, Yamamoto M. Combinatorial Gata2 and Sca1 expression defines hematopoietic stem cells in the bone marrow niche. Proc Natl Acad Sci U S A 2006;103:2202–7. [PubMed: 16461905]

NIH-PA Author Manuscript

NIH-PA Author Manuscript

NIH-PA Author Manuscript


20. Korhonen L, Brannvall K, Skoglosa Y, Lindholm D. Tumor suppressor gene BRCA-1 is expressed by embryonic and adult neural stem cells and involved in cell proliferation. J Neurosci Res 2003;71:769–76. [PubMed: 12605402]
21. Beardsley DI, Kowbel D, Lataxes TA, Mannino JM, Xin H, Kim WJ, Collins C, Brown KD. Characterization of the novel amplified in breast cancer-1 (NABC1) gene product. Exp Cell Res 2003;290:402–13. [PubMed: 14567997]
22. Radvanyi L, Singh-Sandhu D, Gallichan S, Lovitt C, Pedyczak A, Mallo G, Gish K, Kwok K, Hanna W, Zubovits J, Armes J, Venter D, Hakimi J, Shortreed J, Donovan M, Parrington M, Dunn P, Oomen R, Tartaglia J, Berinstein NL. The gene associated with trichorhinophalangeal syndrome in humans is overexpressed in breast cancer. Proc Natl Acad Sci U S A 2005;102:11005–10. [PubMed: 16043716]
23. Kishi Y, Okudaira S, Tanaka M, Hama K, Shida D, Kitayama J, Yamori T, Aoki J, Fujimaki T, Arai H. Autotaxin is overexpressed in glioblastoma multiforme and contributes to cell motility of glioblastoma by converting lysophosphatidylcholine to lysophosphatidic acid. J Biol Chem 2006;281:17492–500. [PubMed: 16627485]
24. Neufeld G, Shraga-Heled N, Lange T, Guttmann-Raviv N, Herzog Y, Kessler O. Semaphorins in cancer. Front Biosci 2005;10:751–60. [PubMed: 15569615]
25. Kirkham DL, Pacey LK, Axford MM, Siu R, Rotin D, Doering LC. Neural stem cells from protein tyrosine phosphatase sigma knockout mice generate an altered neuronal phenotype in culture. BMC Neurosci 2006;7:50. [PubMed: 16784531]
26. Rouzier R, Rajan R, Wagner P, Hess KR, Gold DL, Stec J, Ayers M, Ross JS, Zhang P, Buchholz TA, Kuerer H, Green M, Arun B, Hortobagyi GN, Symmans WF, Pusztai L. Microtubule-associated protein tau: a marker of paclitaxel sensitivity in breast cancer. Proc Natl Acad Sci U S A 2005;102:8315–20. [PubMed: 15914550]
27. Mylona E, Magkou C, Giannopoulou I, Agrogiannis G, Markaki S, Keramopoulos A, Nakopoulou L. Expression of tissue inhibitor of matrix metalloproteinases (TIMP)-3 protein in invasive breast carcinoma: Relation to tumor phenotype and clinical outcome. Breast Cancer Res 2006;8:R57. [PubMed: 17032447]
28. Turnley AM, Faux CH, Rietze RL, Coonan JR, Bartlett PF. Suppressor of cytokine signaling 2 regulates neuronal differentiation by inhibiting growth hormone signaling. Nat Neurosci 2002;5:1155–62. [PubMed: 12368809]
29. Aoki M, Yamashita T, Tohyama M. EphA receptors direct the differentiation of mammalian neural precursor cells through a mitogen-activated protein kinase-dependent pathway. J Biol Chem 2004;279:32643–50. [PubMed: 15145949]
30. Druker BJ, Talpaz M, Resta DJ, Peng B, Buchdunger E, Ford JM, Lydon NB, Kantarjian H, Capdeville R, Ohno-Jones S, Sawyers CL. Efficacy and safety of a specific inhibitor of the BCR-ABL tyrosine kinase in chronic myeloid leukemia. N Engl J Med 2001;344:1031–7. [PubMed: 11287972]
31. Reardon DA, Egorin MJ, Quinn JA, Rich JN, Gururangan S, Vredenburgh JJ, Desjardins A, Sathornsumetee S, Provenzale JM, Herndon JE 2nd, Dowell JM, Badruddoja MA, McLendon RE, Lagattuta TF, Kicielinski KP, Dresemann G, Sampson JH, Friedman AH, Salvado AJ, Friedman HS. Phase II study of imatinib mesylate plus hydroxyurea in adults with recurrent glioblastoma multiforme. J Clin Oncol 2005;23:9359–68. [PubMed: 16361636]
32. van Oosterom AT, Judson I, Verweij J, Stroobants S, Donato di Paola E, Dimitrijevic S, Martens M, Webb A, Sciot R, Van Glabbeke M, Silberman S, Nielsen OS. Safety and efficacy of imatinib (STI571) in metastatic gastrointestinal stromal tumours: a phase I study. Lancet 2001;358:1421–3. [PubMed: 11705489]
33. Takayama N, Sato N, O'Brien SG, Ikeda Y, Okamoto S. Imatinib mesylate has limited activity against the central nervous system involvement of Philadelphia chromosome-positive acute lymphoblastic leukaemia due to poor penetration into cerebrospinal fluid. Br J Haematol 2002;119:106–8. [PubMed: 12358909]
34. Smith AG, Heath JK, Donaldson DD, Wong GG, Moreau J, Stahl M, Rogers D. Inhibition of pluripotential embryonic stem cell differentiation by purified polypeptides. Nature 1988;336:688–90. [PubMed: 3143917]

NIH-PA Author Manuscript

NIH-PA Author Manuscript

NIH-PA Author Manuscript

35. Wright LS, Li J, Caldwell MA, Wallace K, Johnson JA, Svendsen CN. Gene expression in human neural stem cells: effects of leukemia inhibitory factor. J Neurochem 2003;86:179–95. [PubMed: 12807438]

36. Metcalf D. The unsolved enigmas of leukemia inhibitory factor. Stem Cells 2003;21:5–14. [PubMed: 12529546]

37. Palmqvist L, Glover CH, Hsu L, Lu M, Bossen B, Piret JM, Humphries RK, Helgason CD. Correlation of murine embryonic stem cell gene expression profiles with functional measures of pluripotency. Stem Cells 2005;23:663–80. [PubMed: 15849174]

38. Fournier MV, Martin KJ. Transcriptome profiling in clinical breast cancer: from 3D culture models to prognostic signatures. J Cell Physiol 2006;209:625–30. [PubMed: 17001673]

NIH-PA Author Manuscript
NIH-PA Author Manuscript
NIH-PA Author Manuscript



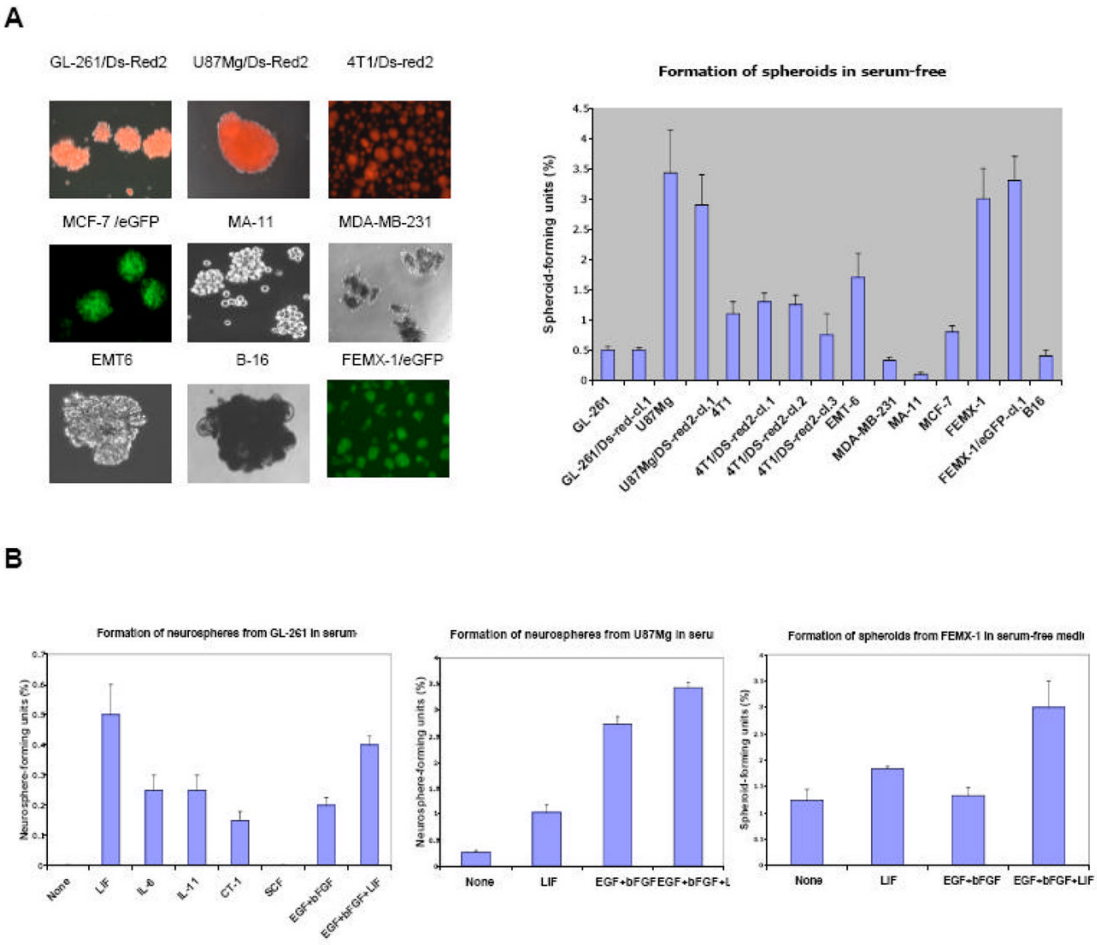


**Figure 1. Growth of cancer cell lines and fluorescent clones as spheroids in serum-free medium (SFM)**

**A.** Left panel: Phase contrast and fluorescence micrographs of spheroids after 7 day-culture of cancer cells in SFM. GL-261, EMT6, 4T1 and FEMX-1 cancer cell lines were transduced with SF91/DsRed2 or SF91/eGFP retroviral vectors and cloned by limiting dilution before being cultured in SFM. Micrographs were obtained with a Zeiss Axiovert 200 M microscope and Axiovision software (10x objective for 4T1/Ds-red2 and FEMX-1/eGFP, 40X objective for EMT6 and B16; 20x objective for all the others); right panel: Percentage of spheroid-forming cells in cancer cell lines and their fluorescent clones. **B.** The effect of various growth factors on the formation of spheroids by GL-261, U87Mg and FEMX-1 cells. LIF, leukemia inhibitory factor; IL-6, interleukin 6; IL-11, interleukin 11; CT-1, cardiotrophin 1; SCF, stem cell factor; EGF, epidermal growth factor; bFGF, basic fibroblast growth factor. Results were reproduced in at least three independent experiments. Results from typical experiments performed in triplicate are shown; bars, SD.

NIH-PA Author Manuscript
NIH-PA Author Manuscript
NIH-PA Author Manuscript



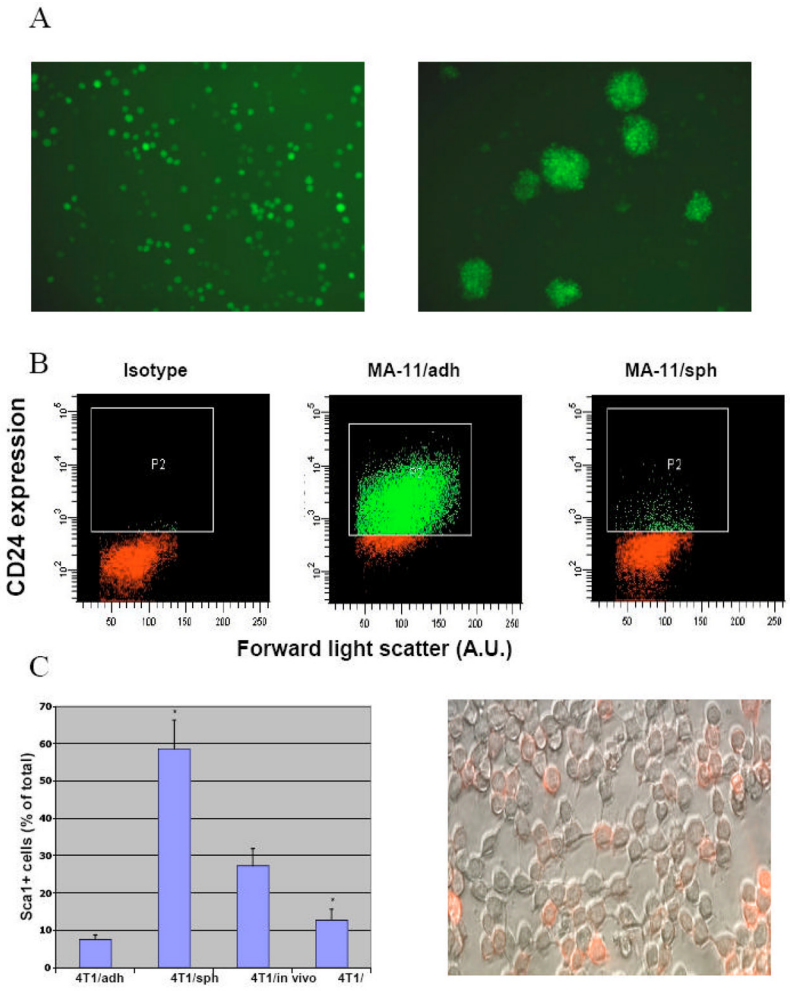


**Figure 2. Characteristics of spheroid-forming cells**

**A.** After 5 days of culture in SFM, the adherent cell fraction and the dissociated spheroids of MCF-7/eGFP cells were separately plated in standard serum-additioned medium for 5 additional days. Both cultures resumed exponential growth. However, when re-plated in SFM, the sph fraction (right panel), but not the adh fraction (left panel) re-formed spheroids (100X magnification); **B.** CD24-positivity by flow cytometry of human MA-11 cells grown in serum-supplemented medium (MA-11/adh) or in serum-free medium (MA-11/sph); P2, gate for CD24 + cells; A.U., arbitrary units; 10,000 events were analyzed for each sample; **C.** Left panel: Sca1-positivity by flow cytometry of 4T1/adh, 4T1/sph and 4T1 cells from s.c. tumors immediately after enzymatic dissociation of the cells (4T1/in vivo) or ex-vivo culture for one week (4T1/ex-vivo). Results were reproduced in at least three independent experiments. Results from a typical experiment performed in triplicate are shown; bars, SD; right panel: Sca1-FITC-positive 4T1 cells were single-cell sorted and cloned. The clones were expanded in culture and analyzed ten days later by immunofluorescence. The resulting clones had a heterogeneous expression of Sca1 (magnification, 200X).

NIH-PA Author Manuscript
NIH-PA Author Manuscript
NIH-PA Author Manuscript



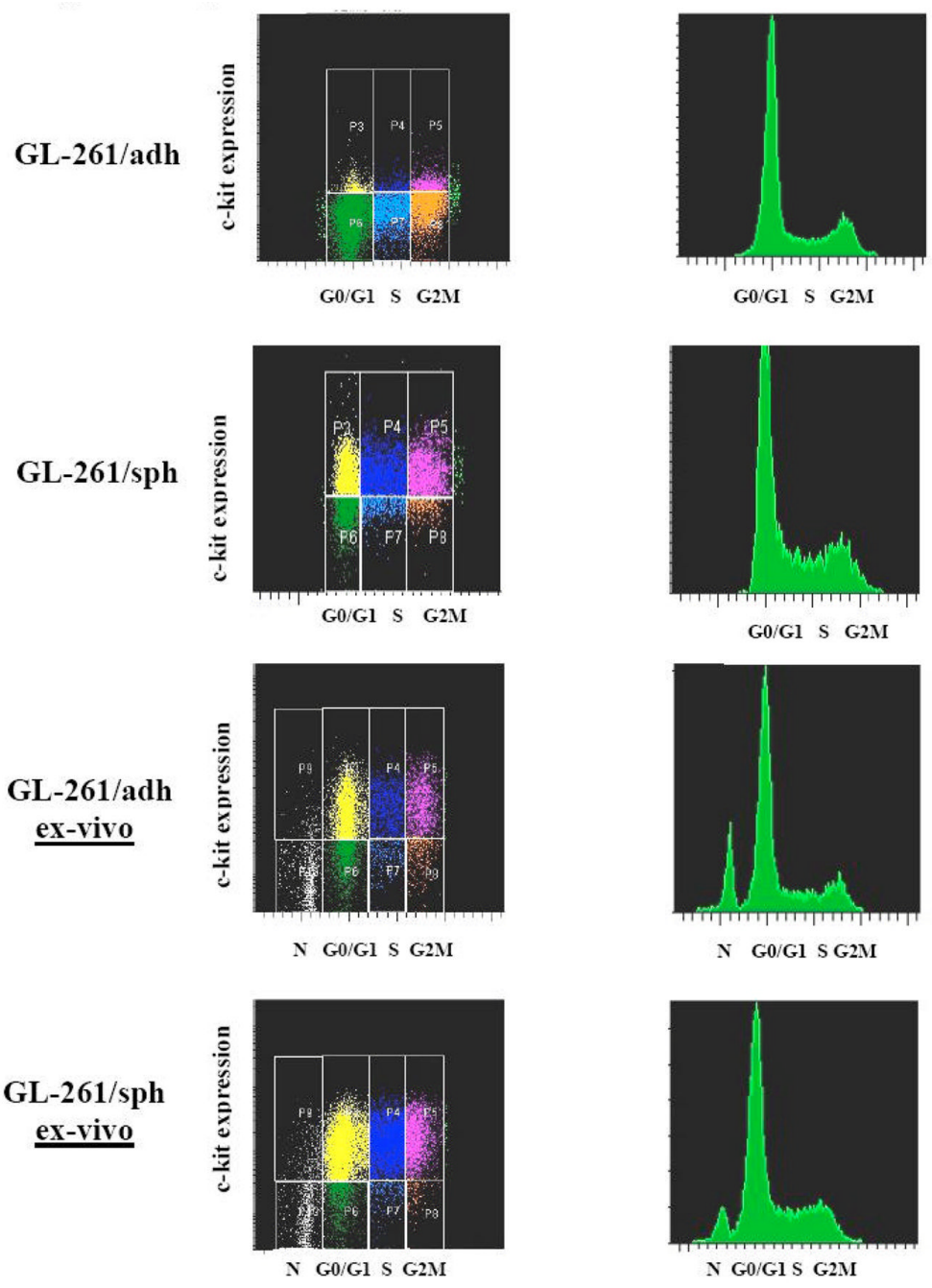


**Figure 3. Flow cytometric analysis of *c-kit* in the different phases of the cell cycle of GL-261/adh, GL-261/sph and of ex-vivo GL-261, dissociated from brain tumors of mice derived from GL-261/adh or GL-261/sph cells**

The supravital DNA stain Hoechst 33342 was employed for cell cycle analysis and to distinguish normal diploid brain cells from hyperdiploid GL-261 cells. P3–P5 and P6–P8 represent gates for *c-kit*-positive cells and *c-kit*-negative cells, respectively, compared with their isotypic control. P3 and P6, cells in G0/G1; P4 and P7, cells in S; P5 and P8, cells in G2-M phases of the cell cycle. N, normal brain cells.

NIH-PA Author Manuscript
NIH-PA Author Manuscript
NIH-PA Author Manuscript



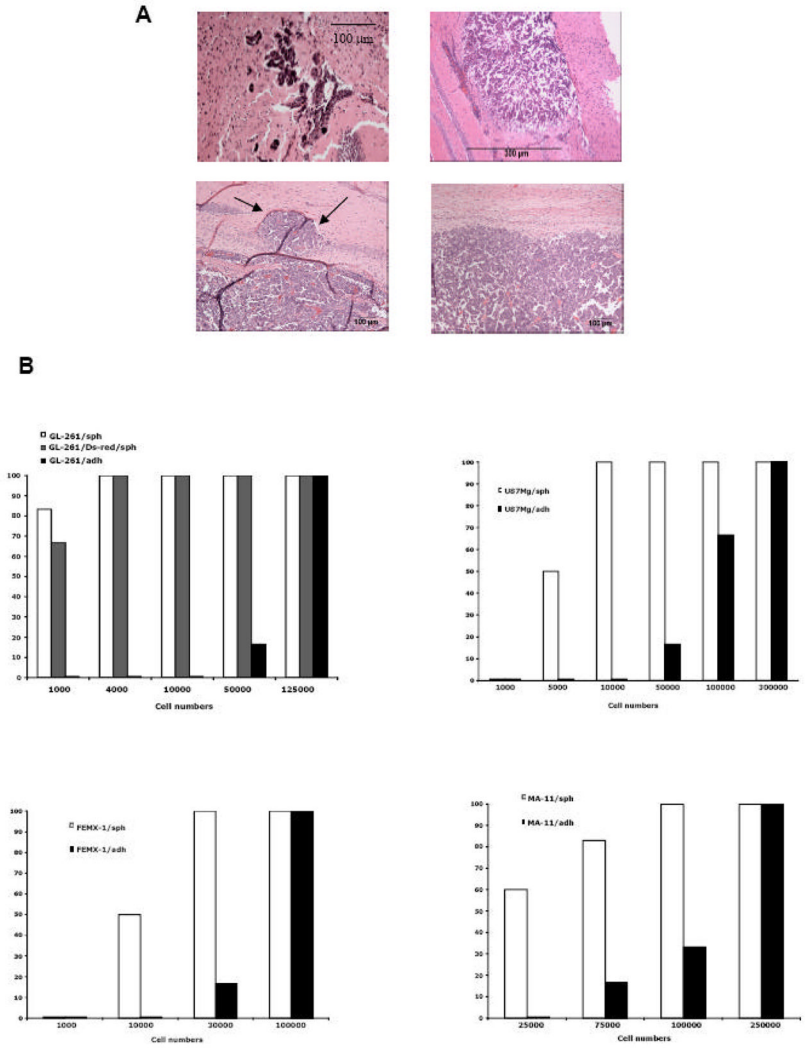


**Figure 4. In vivo studies**

(**A**) Representative H&E-stained sections of brain tumors derived from orthotopic implantation of GL-261 glioma cells in adherence (right panels) or as spheroids in serum-free medium (left panels). Arrows, areas of tumor infiltration into the brain parenchyma. (**B**) In vivo growth of GL-261, U87Mg, FEMX-1 and MA-11 cells in adherence (adh) or as spheroids (sph). GL-261 and U87Mg cells were orthotopically implanted into C57Bl/6 and nu/nu mice, respectively; the percentage of mice (6/cohort) developing an intracranial tumor > 1mm3 after 20 days was calculated. Human FEMX-1 melanoma and MA-11 breast carcinoma cells were implanted s.c. into the right flank of nu/nu mice; the percentage of mice (6/cohort) developing a tumor > 500 mm3 after 30 days (FEMX-1) and 70 days (MA-11) was calculated.

NIH-PA Author Manuscript

NIH-PA Author Manuscript

NIH-PA Author Manuscript

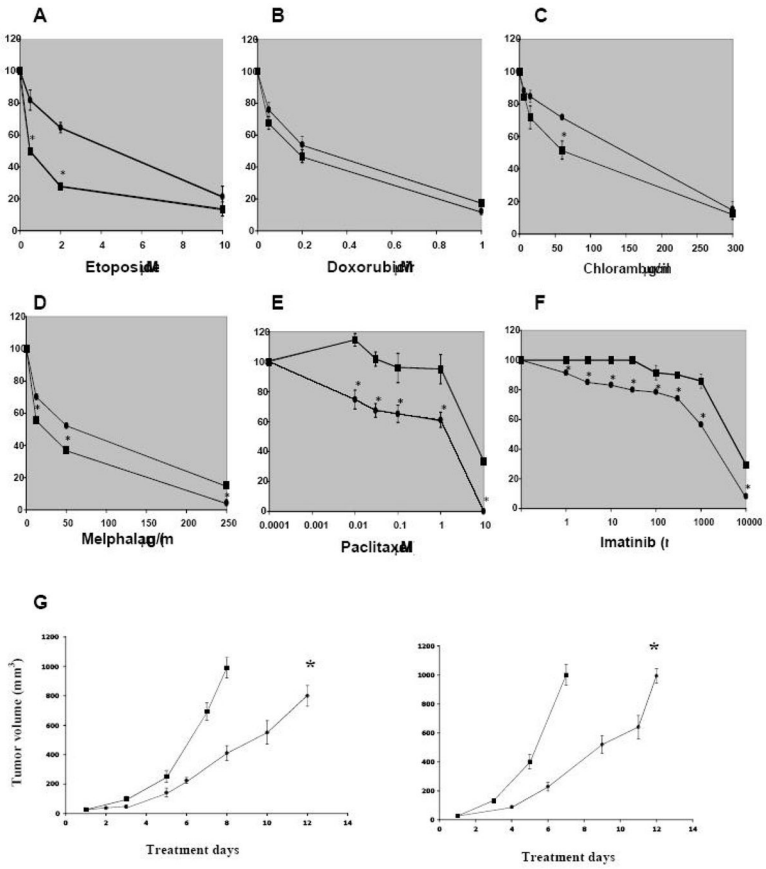


**Figure 5. Differential sensitivity of GL-261 grown in adherence (○) or as spheroids (□) to the cytotoxic activity of anticancer compounds in vitro and in vivo**

**A–F:** After 3 days of continuous exposure, the sensitivity of cells to the various drugs was measured by the MTS/PMS assay and expressed as a percent of the absorbance value of cells treated with the solvent alone (ranging from 1.0 to 1.5 $\Delta A_{490nm}$). Results were reproduced in at least three independent experiments. Results from a typical experiment performed in triplicate are shown; bars, SD (shown only when they are larger than the points). *, $p<0.05$, significant difference from control. G: Subcutaneous tumor growth under imatinib therapy in GL-261/adh (left panel) and GL-261/sph (right panel) tumor-bearing mice. Mice (6/group) were treated i.p. once a day for 14 days. Treatment was initiated when the tumors reached a size of approximately 25 $mm^3$. (□), PBS control; (○) 50 mg/Kg imatinib. *, $P<0.05$, significantly different compared with the control group.

NIH-PA Author Manuscript

NIH-PA Author Manuscript

NIH-PA Author Manuscript

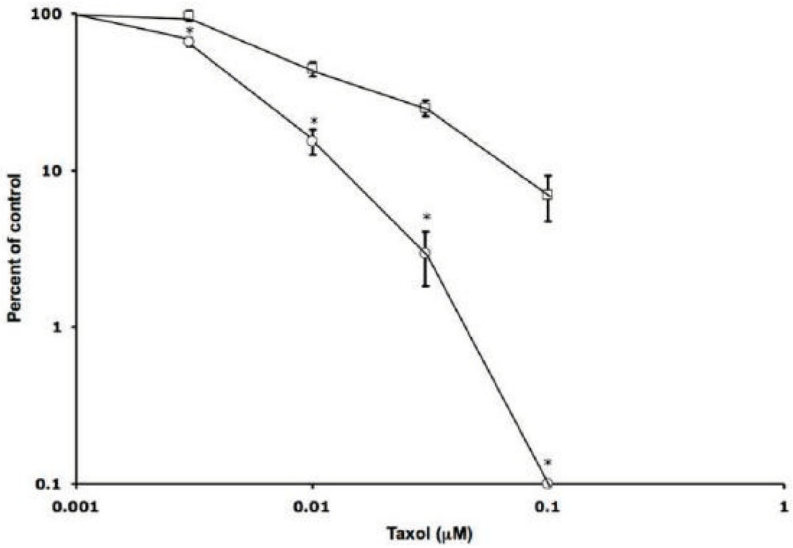


**Figure 6. Clonogenic assay for GL-261 cells grown in adherence (○) or as spheroids (□) exposed to the cytotoxic activity of taxol**

After 7 days of continuous exposure, the sensitivity of cells to taxol was measured by a clonogenic assay and expressed as a percent of cells treated with the solvent alone. Points represent the mean of three experiments performed in duplicate; bars, SE (shown only when they are larger than the points). *, $p<0.05$, significant difference from control.

NIH-PA Author Manuscript

NIH-PA Author Manuscript

NIH-PA Author Manuscript

**Table 1**

Cells were plated in serum-supplemented medium at clonal density (100/cm2), and their clonogenic (plating) efficiency determined by counting the number of colonies containing more than 50 cells after 7 days of culture. The adherent colonies (adh) were then dissociated by trypsin-EDTA, and plated in serum-free medium. Sphere formation was quantitated after 7 days. Data are the mean ± SD of three separate experiments.

| Cell line | Plating efficiency | Sphere formation from adh colonies |
|---|---|---|
| U87MG | 19.0 ± 0.5 | 2.5 ± 1 |
| MA-11 | 32.6 ± 4.5 | 0.4 ± 0.2 |
| FEMX-1 | 56.3 ± 9.9 | 3.2 ± 1.1 |